

# A plastic damage mechanics model for Engineered Cementitious Composites

L. Dick-Nielsen, H. Stang & P. N. Poulsen

*Department of Civil Engineering, The Technical University of Denmark, Lyngby, Denmark*

P. Kabele

*Faculty of Civil Engineering, Czech Technical University in Prague, Czech Republic*

**ABSTRACT:** This paper discusses the establishment of a plasticity-based damage mechanics model for Engineered Cementitious Composites (ECC). The present model differs from existing models by combining a matrix and fiber description in order to describe the behavior of the ECC material. The model provides information about crack opening and spacing, which makes it possible to assess the condition of a structure in the serviceability state. A simulation of a four point bending beam is performed to demonstrate the capability of the model.

## 1 INTRODUCTION

Engineered Cementitious Composites (ECC) is a strain-hardening fiber reinforced cementitious composite (Li and Leung 1992). In contrast to conventional Fiber Reinforced Concrete (FRC), ECC is characterized by its ability to undergo multiple cracking in tension. Conceptually, the cementitious matrix in ECC is assumed to contain initial flaws, which are randomly distributed throughout the composite material. When the material is loaded in tension, micro-cracks are initiated from the initial flaws due to stress concentrations at the tip of the flaws. The formation and propagation of micro-cracks is taking place under increasing load and gives rise to multiple cracking and strain-hardening. To assess the state of the material in the serviceability state, information about the crack opening and spacing is required and a plasticity-based damage mechanics model providing such information is presented.

Due to the strain hardening behavior of the ECC material, smeared crack models available in commercial Finite Element Method (FEM) programs are often used to simulate the behavior of ECC structures (Walter, Olesen, Stang, and Vejrum 2006) and (Dick-Nielsen, Stang, and Poulsen 2006b). An overview of smeared models is given by (Jirasek 2004). An example of a model specifically developed for ductile fiber-reinforced cement-based composite like ECC is (Han, Feenstra, and Billington 2003). This model is a total strain, rotating smeared crack model. The model is characterized by its detailed description of the unloading

phase, which makes it suitable for cyclic loading simulations. In the ECC model proposed by (Kabele 2002) the cracks are fixed when initiated. The model is characterized by the scheme used to describe the stiffness of the fibers in the direction parallel with the crack surface, where the fibers are described as randomly orientated elastic Timoshenko beams. In the latter model the behavior of the cracks after initiation is described solely through the fibers.

A series of finite element simulations on the micro and meso scale has been carried out in previous investigations by the authors. These simulations were performed to get a better understanding of the strain-hardening process in ECC. On the micro scale, the mechanism during micro-crack propagation and subsequently fiber debonding and pull-out were investigated (Dick-Nielsen, Stang, and Poulsen 2005). On the meso scale, investigations on the propagation of single and multiple cracks were performed (Dick-Nielsen, Stang, and Poulsen 2006a) and (Stang, Olesen, Poulsen, and Dick-Nielsen 2006). The present paper describes the establishment of a plasticity-based damage mechanics model on the macro scale.

The present model is based on the smeared fixed, multiple cracking approach. The model differs from existing models by combining a matrix and fiber description in order to describe the behavior of the ECC material. This model is meant for use in the serviceability state. In this state the crack openings would be in the orders of 40-50  $\mu\text{m}$ . A realistic description of the ECC material for these crack openings should

therefore include the matrix behavior as well as the fiber behavior as shown in (Dick-Nielsen, Stang, and Poulsen 2005) and (Dick-Nielsen, Stang, and Poulsen 2006a).

The matrix is described by employing an elasto-plastic material model for crack initiation and propagation in plain concrete. The model is a mixed mode cohesive crack model combined with a modified Mohr-Coulomb yield-surface. Even though the fracture energy of the ECC matrix is low, it is shown in (Stang, Olesen, Poulsen, and Dick-Nielsen 2006) that it is best described by a cohesive approach. The matrix model employed in this paper is a modified version of the model originally developed by (Carol, Prat, and López 1997). During sliding of a crack the model is able to capture the dilatation in the normal direction.

The stiffness of the fibers in the normal direction to the crack surface is described through a multi-linear strain-stress curve, which can be found from a uniaxial tensile test. While the stiffness of the fibers parallel to the crack surface is described as randomly orientated Timoshenko beams bridging the crack (Kabele 2002).

## 2 PLASTICITY DAMAGE MODEL

A 2D representative volume element (RVE) in plane stress with the side length,  $l$  is considered. It is assumed that this RVE can be considered as a material point, where the constitutive equations are solved. The RVE is subjected to average total stress,  $\sigma$  and strain,  $\varepsilon$ , and can contain series of parallel multiple cracks, where each series have different orientation. In this section the constitutive equations for a RVE containing multiple cracks in multiple crack directions will be derived for the plastic and elastic state.

### 2.1 Model input

As input to the model, information concerning the ECC-level, the fibers and the matrix are required.

On the ECC-level the following data are needed: the initial E-modulus,  $E_0$ , Poisson's ratio,  $\nu$ , the tensile strength,  $f_{t,ECC}$ , a constant,  $b$  that determines the crack opening at which the crack becomes stress free during unloading and the threshold angle between two crack directions in one iteration point,  $\phi$ . A small angle between two crack directions would be a numerical and not physical phenomenon, why the threshold angle should not be too small. The relationship between total strain,  $\varepsilon$  and stress,  $\sigma$  (fig. 1) is required. This relationship can be found from a uniaxial tensile test or through a bending test and an inverse analysis (Østergaard 2003). The uniaxial tensile curve obtained from test is usually jagged (Wang and Li 2004). To avoid numerical problems during computations an idealized smooth curve is employed as shown in the

figure. Finally the relationship between the total normal strain and the numbers of parallel cracks,  $N$  in the RVE (fig. 2,  $n = N/l$ ) is needed. Since a smooth overall stress strain response is aimed for, the latter curve has to be continuous. This means that the number of cracks per length,  $n$  increases linearly as a function of the strain in the crack direction. It is assumed that all cracks in one direction associated with one integration point has identical crack opening,  $\delta$ .

For the fibers the following input is needed: a shear stiffness constant,  $k$ , which gives the relationship between crack opening and bridging stress. This constant depend on the fiber volume fraction,  $V_f$ , the shear modulus for the fibers,  $G_f$  and the shape of the fibers (Kabele 2002). The shear stiffness constant will be calibrated through experiments.

The material parameters required for the matrix are the tensile strength,  $f_t$ , the cohesion,  $c$ , two friction coefficients for the yield surface,  $\mu_f$  and  $\mu_0$ , a friction coefficient for the plastic potential,  $\mu_g$  and the mode I and II fracture energy,  $G_{F,I}$  and  $G_{F,II}$ .

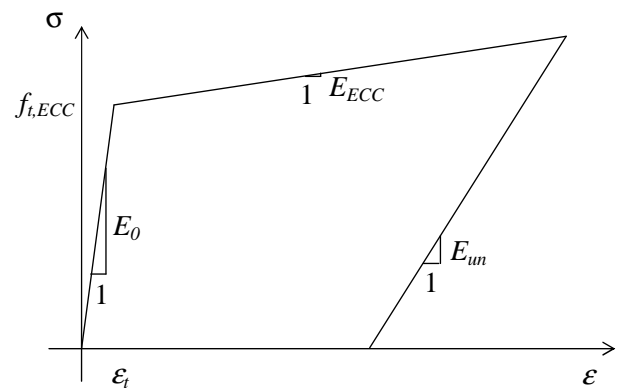


Figure 1: Constitutive relationship for ECC.

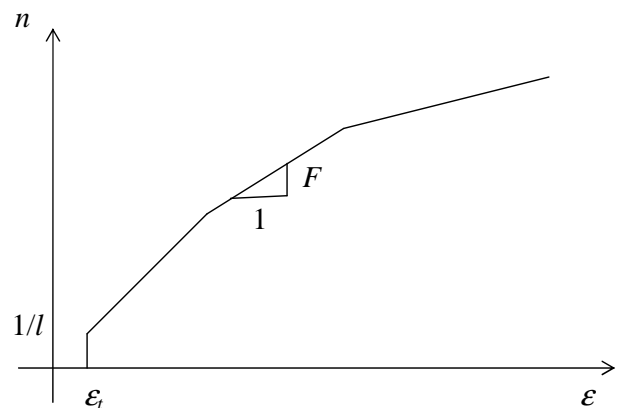


Figure 2: Damage law: strain vs. crack number per length,  $n$ .

### 2.2 The constitutive equations

The first crack is initiated when the stress state in the mortar reaches the yield-surface. The normal to the crack surface is parallel with the normal stress that

initiated the crack and the crack direction remains fixed. Due to equilibrium the stress,  $\sigma$ , is equal to the stress in the crack,  $\sigma_{cr}$  and the stress in the uncracked elastic part of the material,  $\sigma_e$ :

$$\sigma = \sigma_{cr} = \sigma_e \quad (1)$$

The strain,  $\varepsilon$  can be split into two parts, one related to the uncracked elastic material,  $\varepsilon_e$  and one related to the additional deformations due to opening of cracks,  $\varepsilon_{cr}$ :

$$\varepsilon = \varepsilon_e + \varepsilon_{cr} \quad (2)$$

In fig. 3 a local coordinate system is shown in a crack. The relationship between the global strain in a crack,  $\varepsilon_{cr}$  and the local strain increment in a crack,  $e_{cr}$  can be written as:

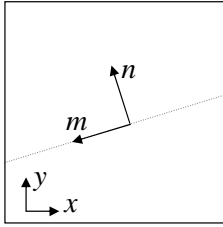


Figure 3: Local coordinate system in crack.

$$\varepsilon_{cr} = \mathbf{T} e_{cr} \quad (3)$$

$$\begin{bmatrix} \varepsilon_x^{cr} \\ \varepsilon_y^{cr} \\ \gamma_{xy}^{cr} \end{bmatrix} = \begin{bmatrix} n_x^2 & n_x m_x \\ n_y^2 & n_y m_y \\ 2n_x n_y & n_x m_y + n_y m_x \end{bmatrix} \begin{bmatrix} \varepsilon_{nn}^{cr} \\ \gamma_{nm}^{cr} \end{bmatrix} \quad (4)$$

where  $\mathbf{T}$  is the transformation matrix. A similar relationship can be found between the global stress,  $\sigma$  and the traction,  $s$  in the crack:

$$s = \mathbf{T}^T \sigma \quad (5)$$

The relationship between the local strain in the crack,  $e_{cr}$ , the crack opening for a single crack,  $\delta$ , the length of the RVE,  $l$  and the number of parallel cracks in the RVE,  $N$  can be written as:

$$e_{cr} = N/l\delta = n\delta \quad (6)$$

where  $n$  is the number of parallel cracks per length. Thus the total strain formulation (eq. 2) can then be rewritten as:

$$\varepsilon = \varepsilon_e + \mathbf{T}n\delta \quad (7)$$

In incremental form the split of strain gives:

$$d\varepsilon = d\varepsilon_e + \mathbf{T}dn\delta + \mathbf{T}nd\delta \quad (8)$$

The relationship between the elastic strain increment,  $d\varepsilon_e$  and stress increment,  $d\sigma$  is:

$$d\sigma = D_e d\varepsilon_e = D_e(d\varepsilon - \mathbf{T}dn\delta - \mathbf{T}nd\delta) \quad (9)$$

where  $D_e$  is the elastic stiffness matrix. This matrix refer to the intact material between the cracks and is therefore constant through out the entire analysis.

$$D_e = [\mathbf{C}_e]^{-1} = \frac{E_0}{1-\nu^2} \begin{bmatrix} 1 & \nu & 0 \\ \nu & 1 & 0 \\ 0 & 0 & \frac{1-\nu}{2} \end{bmatrix} \quad (10)$$

The relationship between crack opening for a single crack,  $\delta$  and traction in the crack,  $s$  in incremental form can be written as:

$$d\delta = \mathbf{C}_{cr} ds = \mathbf{C}_{cr} \mathbf{T}^T d\sigma \quad (11)$$

where the traction,  $ds$  is substituted by use of eq. 5 and  $\mathbf{C}_{cr}$  is the tangent compliance matrix for a single crack. In order to solve the differential equation (eq. 9) we need to introduce the damage law in incremental form:

$$dn = F(\varepsilon_{nn})d\varepsilon_{nn} \quad (12)$$

where  $d\varepsilon_{nn}$  is the normal component of total strain in the crack direction ( $d\varepsilon_{nn} = [1 \ 0] \mathbf{T}^T d\varepsilon$ ) and  $F$  is the slope of the damage law (see fig. 2). Inserting eq. 11 and 12 in eq 9 the differential equation can now be written as:

$$d\sigma = D_e(d\varepsilon - \mathbf{T}F d\varepsilon_{nn}\delta - \mathbf{T}n\mathbf{C}_{cr}\mathbf{T}^T d\sigma) \quad (13)$$

In order to obtain a relationship between total strain increment,  $d\varepsilon$  and the stress increment,  $d\sigma$  a rearranging of eq. 13 is performed:

$$(\mathbf{C}_e + \mathbf{T}n\mathbf{C}_{cr}\mathbf{T}^T)d\sigma = (d\varepsilon - \mathbf{T}F\delta d\varepsilon_{nn})$$

$$(\mathbf{C}_e + \mathbf{T}n\mathbf{C}_{cr}\mathbf{T}^T)d\sigma = (\mathbf{I} - \mathbf{T}F\delta[1 \ 0]\mathbf{T}^T)d\varepsilon$$

$$d\sigma = (\mathbf{C}_e + \mathbf{T}n\mathbf{C}_{cr}\mathbf{T}^T)^{-1}(\mathbf{I} - \mathbf{T}F\delta'\mathbf{T}^T)d\varepsilon \quad (14)$$

where  $\mathbf{I}$  is a 3 by 3 unit matrix and  $\delta'$  is a 2 by 2 matrix containing the displacement components:

$$\delta' = \begin{bmatrix} \delta_{nn} & 0 \\ \delta_{mn} & 0 \end{bmatrix} \quad (15)$$

The tangent stiffness matrix,  $D_{ep}$ , is readily identified from eq. 14. For multiple crack directions  $\mathbf{T}$ ,  $n\mathbf{C}_{cr}$  and  $F\delta'$  can be written as:

$$\mathbf{T} = [ \mathbf{T}_1 \quad \mathbf{T}_2 \quad \dots \quad \mathbf{T}_j ] \quad (16)$$

$$n\mathbf{C}^{cr} = \begin{bmatrix} n_1\mathbf{C}_1^{cr} & 0 & \dots & 0 \\ 0 & n_2\mathbf{C}_2^{cr} & & 0 \\ \vdots & & & \vdots \\ 0 & 0 & \dots & n_j\mathbf{C}_j^{cr} \end{bmatrix} \quad (17)$$

$$F\boldsymbol{\delta}' = \begin{bmatrix} F_1\boldsymbol{\delta}'_1 & 0 & \dots & 0 \\ 0 & F_2\boldsymbol{\delta}'_2 & & 0 \\ \vdots & & & \vdots \\ 0 & 0 & \dots & F_j\boldsymbol{\delta}'_j \end{bmatrix} \quad (18)$$

where  $j$  refer to the current crack direction.

### 2.3 Matrix model

The matrix is modelled employing an elasto-plastic material model for crack initiation and propagation in plain concrete. The employed model is a modified version of the model originally developed by (Carol, Prat, and López 1997). The model is a mixed mode cohesive crack model combined with a modified Mohr-Coulomb yield-surface,  $f$ :

$$f = (s_{mn}^m)^2 - (c - s_{nn}^m\mu)^2 + (c - f_t\mu)^2, \quad (19)$$

where  $s_{mn}^m$  is the traction in the matrix,  $c$  is the cohesion,  $\mu$  is the friction coefficient and  $f_t$  is the tensile strength of the matrix. During sliding of a crack the model is able to capture the dilatation in the normal direction. The dilatation phenomenon is essential when modelling crack propagation in cementitious materials. If a crack opening is confined in the normal direction during sliding, large compression normal forces can be build up in the structural member. If the model does not capture this phenomenon the carrying capacity of the structural member can be underestimated. The model includes damage parameters and as the material softens the shape of the yield-surface will gradually tend towards the Coulomb yield-surface. The Coulomb yield-surface eventually models friction between two separate surfaces due to a non-associated flow rule (eq. 20), which represents the plastic potential:

$$g = (s_{mn}^m)^2 - (c - s_{nn}^m\mu_g)^2 + (c - f_t\mu_g)^2, \quad (20)$$

Fig. 4 illustrates the traction evolution in a matrix crack for a material point. The crack is initiated under a pure mode I loading condition. After the crack

is initiated the crack is opened in a mixed mode with at tangential opening that is proportional and twice as large as the normal opening. The thick line is the traction path and the thin curves illustrate the evolution of the yield surface from  $f_0$  to  $f_2$ .

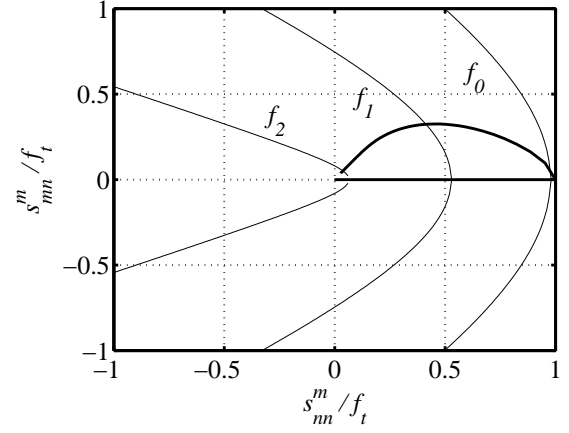


Figure 4: Evolution of traction and yield-surface in the matrix under mixed mode crack opening, where  $s$  is matrix traction and  $f_0$  and  $f_2$  are the initial and final yield-surface respectively.

### 2.4 Fiber model

The stiffness of the fibers in the direction normal to the crack surface,  $E_b$  is found through information of the global normal stiffness of the ECC,  $E_{ECC}$ , the initial E-modulus for plane stress,  $E = E_0/(1 - \nu^2)$ , the number of parallel cracks per length,  $n$  and the stiffness of the matrix for pure mode I opening,  $E_{nn,I}^m$ . By considering only the stiffness in the direction normal to a crack eq. 14 gives us:

$$(1/E + nC_{11}^{cr})^{-1}(1 - F\delta_{nn}) = E_{ECC} \quad (21)$$

By substituting the crack compliance,  $C_{11}^{cr}$  with the sum of the mode I matrix and fiber stiffness,  $C_{11}^{cr} = 1/(E_b + E_{nn,I}^m)$ , the mode I fiber stiffness,  $E_b$  can be found:

$$E_b = \frac{nE_{ECC}E + E_{nn,I}^m(E_{ECC} - E + E\delta_{nn}F)}{E - E_{ECC} - E\delta_{nn}F} \quad (22)$$

where the pure mode I stiffness of the matrix,  $E_{nn,I}^m$  is found as a function of the current normal opening of a single crack. Due to the present formulation the global tangent stiffness computed agrees with the global tangent stiffness,  $E_{ECC}$  found from an idealization of an uniaxial tensile test, when the cracks open in pure mode I. If the cracks open in mixed mode the actual normal stiffness for the matrix,  $E_{nn}^m$  will be lower than the pure mode I stiffness,  $E_{nn,I}^m$  due to

the mixed mode crack formulation. It is assumed that the fiber normal stiffness,  $E_b$  is unaffected by mixed mode crack opening.

During sliding of a crack the fibers are modelled as randomly orientated Timoshenko beam and the relationship between crack deformations and shear stresses are found by solving a boundary value problem (Kabele 2002):

$$s_{nm}^b = k \frac{\delta_{nm}}{\delta_{nn}} \quad (23)$$

where  $k$  is a constant calibrated by test, and  $\delta_{nn}$  and  $\delta_{nm}$  are the mode I and II opening of the crack. The tangent stiffness matrix for the fibers can then be written as:

$$D_{cr}^b = \begin{bmatrix} E_b & 0 \\ -\frac{k\delta_{nm}}{\delta_{nn}^2} & \frac{k}{\delta_{nn}} \end{bmatrix} \quad (24)$$

The stiffness of the fibers,  $D_{cr}^b$  is a smeared stiffness over the crack length.

### 2.5 The total compliance crack matrix

Due to the fact that the matrix and fiber bridging in the crack works in parallel, the total stiffness of the crack can be written as:

$$D_{cr} = D_{cr}^b + D_{cr}^m \quad (25)$$

The superposition of stiffness only holds because the fiber volume concentration,  $V_f$  is small and because the fiber bridging stiffness is a smeared stiffness over the crack length. The superposition of stiffness in the crack remains a hypothesis until the model has been validated by experimental results.

### 2.6 Un- and reloading

During un- and reloading three different elements need to be considered: matrix, fibers and ECC.

Un- and reloading of the matrix is controlled by the yield surface. As observed in experiments (Kesner and Billington 1998) the elastic E-modulus tends to degrade as a function of the largest crack opening obtained. During un- and reloading of the matrix a simple scheme taken this degrading of normal stiffness into consideration is employed (see fig. 5 and eq. 26).

$$E_{nn,unload}^m = \begin{cases} s_{nn}^{m,pl} / ((1-b)\delta_{max}) & \delta_{nn} > b\delta_{max} \\ 0 & b\delta_{max} > \delta_{nn} > 0 \\ \infty & \delta = 0 \end{cases} \quad (26)$$

where  $b$ , is a constant calibrated by experiments,  $s_{nn}^{m,pl}$  is the normal traction before unloading and  $\delta_{max}$  is the maximal normal crack opening before unloading.

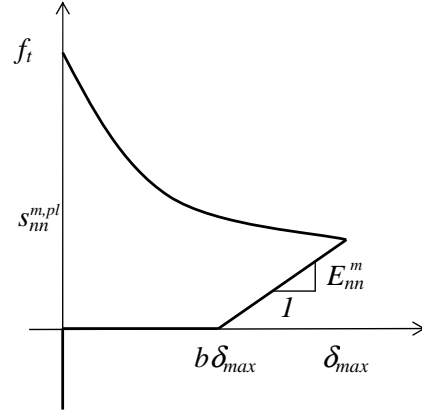


Figure 5: Un- and reloading of matrix.

The normal crack opening,  $\delta_{nn}$  can not assume negative values, because this means that the crack surfaces would overlap. Giving the crack infinitely normal stiffness causes the stiffness of the ECC material in the crack normal direction to be equal to the initial stiffness in compression. Eq. 26 is only valid when unloading occur while the normal traction is positive. If the normal traction is negative before unloading (this can occur during sliding) then the normal-stiffness will be equal to infinity because the matrix is then under compression. If the normal traction becomes positive eq. 26 will again be valid. In order for the traction point to be able to move quickly from one side of the yield surface to the other ( $(s_{nn}^m, s_{nm}^m) \rightarrow (s_{nn}^m, -s_{nm}^m)$ ) when the tangential displacement increment change direction, the elastic shear stiffness for the matrix is set to  $f_t / (1 \mu m)$ . The size of the elastic shear stiffness has influence on the distribution of shear stresses between matrix and fibers in the elastic state. An experimental investigation of this phenomenon can decide the real size.

Un- and reloading of the fibers are controlled by the crack opening. The scheme chosen to determine the relationship between the crack opening and the bridging stiffness normal to the crack surface resemble the one chosen for the matrix (fig. 5). The fibers become elastic when the normal crack opening decreases:

$$E_{nn,unload}^b = \begin{cases} s_{nn}^{b,pl} / ((1-b)\delta_{max}) & \delta_{nn} > b\delta_{max} \\ 0 & b\delta_{max} > \delta_{nn} > 0 \end{cases} \quad (27)$$

When the crack is closed the normal traction is transferred entirely through the matrix. It is assumed for simplicity that the fiber bridging stress can not become negative. When the crack normal opening reaches the previous maximal opening,  $\delta_{max}$ , the bridging stiffness normal to the crack surface is given by eq. 22. It is assumed that the stiffness parallel with the crack surface can be found by use of eq. 23.

Un- and reloading on the ECC level is governed by

the total normal strain in the crack normal direction. If the normal strain decreases the numbers of cracks per length,  $n$  remains constant. When the normal strain in the crack normal direction exceeds the previous maximal strain in the crack normal direction, the ECC becomes plastic and the numbers of cracks per length,  $n$  can again increase.

### 2.7 Initiation of second crack direction

The first crack is initiated when the stress state in the matrix reaches the yield-surface. The normal to the crack surface is parallel with the normal stress that initiated the crack and after crack initiation the crack direction remains fixed. An angle threshold around the first crack where new crack directions can not be initiated is introduced. A second crack direction is initiated when the stress state in the matrix outside the angle threshold reaches the yield-surface. The angle threshold ensures that two crack directions in one integration point will not be initiated with too small an angle separating them, which would be a purely numerical phenomenon.

## 3 FPB SIMULATION

The model is implemented in a user supplied routine in the commercial FEM package 'DIANA'. A simulation of a four point bending (FPB) beam is performed as a test of the present model (see fig. 6). Corresponding experimental results can be found in (Østergaard, Walter, and Olesen 2005). For the simulation a 70 by 17 element mesh is employed. The elements employed are, 8 node, quadrilateral isoparametric plane stress elements. The elements are based on quadratic interpolation and Gauss integration. The dimensions of the beam are: length 500 mm, height 60 mm and width 100 mm. The beam is simply supported and loaded as shown in the figure. Point A and B are used for measuring of vertical displacement,  $u$  and point C will be used to evaluate the state of the material.

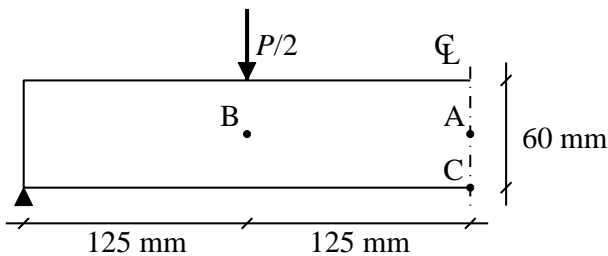


Figure 6: Four point bending beam.

### 3.1 Model input

The material data is found from the FPB experiments and an inverse analysis (Østergaard, Walter, and Olesen 2005): the tensile strength,  $f_{t,ECC} = 2.6$  MPa, the initial E-modulus,  $E_0 = 33$  MPa, the strain-hardening E-modulus,  $E_{ECC} = 0.24$  MPa and the ultimate strain

before softening,  $\varepsilon_u = 0.007$ . After the ultimate strain is reached in the crack normal direction, the normal traction is assumed to decrease linearly until a crack opening of 12 mm is reached. Poisson's ratio,  $\nu$  is assumed to be 0.2.

In order to obtain information about crack opening and spacing from the simulation, information about numbers of cracks per length,  $n$  as a function of the total normal strain in the crack normal direction,  $\varepsilon_{nn}$  are required (see fig. 2). These data was not measured in the experiments, therefore some reasonable values are given as input. Because the cracks are mainly opened in mode I these additional input data will only have little influence on global results like global stresses and deflection of the beam. The relation between the numbers of cracks per length,  $n$  and strain,  $\varepsilon_{nn}$  are chosen as:  $(\varepsilon_{nn}; n [\text{mm}^{-1}])$ ,  $(7.9 \cdot 10^{-5}; 0.1)$ ,  $(1 \cdot 10^{-4}; 0.2)$ ,  $(1 \cdot 10^{-3}; 0.3)$ ,  $(3 \cdot 10^{-3}; 0.4)$  and  $(6 \cdot 10^{-3}; 0.5)$ . Finally the matrix properties related to the elasto-plastic matrix model are chosen as: the matrix tensile strength,  $f_t = 2.0$  MPa, the friction coefficient,  $c = 2.6$  MPa, the mode I fracture energy,  $G_{f,I} = 30$  N/m, the mode II fracture energy,  $G_{f,II} = 30$  N/m, the friction coefficients  $\mu_f = 0.4$ ,  $\mu_0 = 0.75$  and  $\mu_g = 0.375$  and the unloading constant  $b = 0.5$ .

### 3.2 Simulation results

In fig. 7 the load-deflection curve from the simulation is plotted together with the upper and lower bound from the experiments. In contrast to the experiments a partial unloading is performed in the simulation to demonstrate the capability of the model. The load is applied in three steps: first the load is increased until a deflection of approximately 0.7 mm is reached (load point a), then a partial unloading is performed (load point b) and finally the load is increased in the remaining simulation. As shown in the figure the model is able to reproduce the experimental results very well.

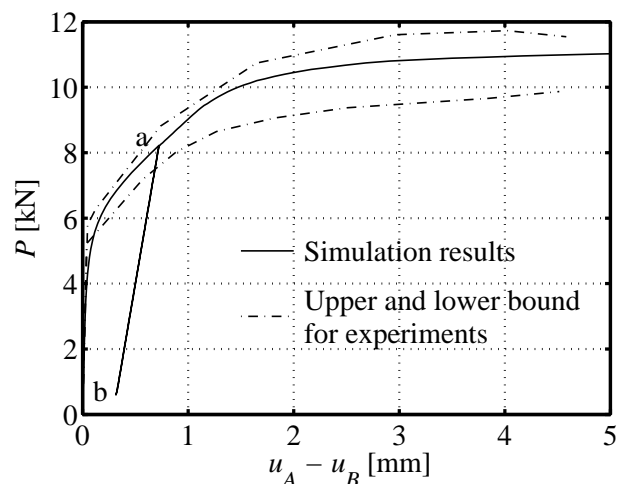


Figure 7: Load deflection curve.

In fig 8 the relationship between the traction,  $s$  in the normal crack direction at point C vs. the relative deflection are shown. The total traction,  $s$  reaches a peak at a relative deflection of approximately 1 mm. After the peak point is reached the ECC material begins to soften. At crack initiation there is a difference between the traction in the ECC material,  $s$  and the traction in the matrix,  $s_m$ . This is in good agreements with observation made in simulations (Dick-Nielsen, Stang, and Poulsen 2005), where a crack with an opening of only a few nano meter runs through the matrix before debonding of the fibers take place. Similar experimental observations has been made by (Wang and Li 2004). The ECC mix 3 in these experiments had a first crack strength of 4 MPa, while experiments performed by Wang at The Technical University of Denmark, showed that the matrix in mix 3 had a tensile strength of 2.83 MPa. As the crack at point C opens the matrix traction begins to soften while the average fiber traction begins to increase. At a relative deflection of approximately 4 mm the crack is only bridged by the fibers. The unloading scheme works as intended, leaving a permanent plastic deformation after unloading.

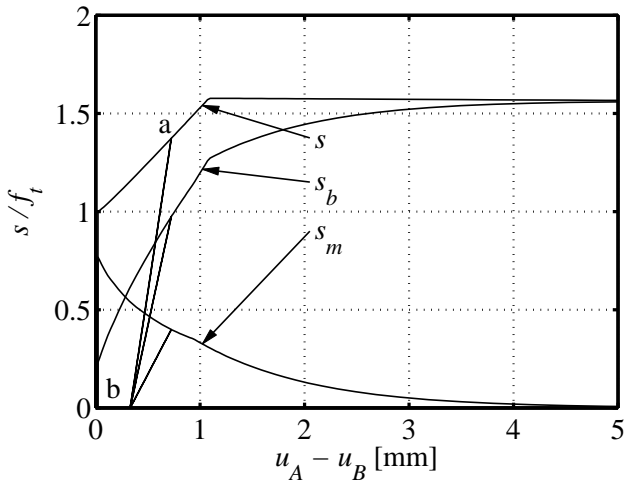


Figure 8: Total traction,  $s$ , fiber bridging traction,  $s_B$  and matrix traction,  $s_m$  in the normal crack direction at point C vs. deflection.

Fig. 9 shows the crack pattern at a deflection of approximately 0.9 mm before localization take place in the bottom of the beam. The line thickness corresponds to the crack opening. Cracks along the entire bottom in the middle section is about to localize, due to the constant moment in this section.

Fig 10 shows the relationship between the relative deflection and the average normal crack opening,  $\delta_{nm}$  at point C. The slope of the curve changes after a deflection of 1 mm, which is the point at which softening begins to take place in the bottom of the beam. At a relative deflection of 5 mm the average crack opening at point C is  $70 \mu m$ . During unloading from loading

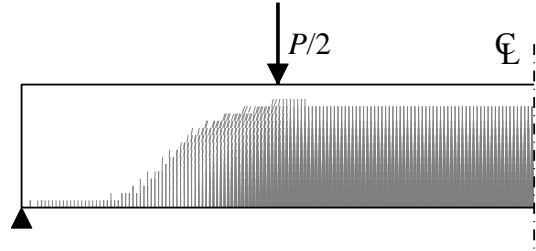


Figure 9: Crack pattern in the beam at a deflection of 0.9 mm. The line thickness corresponds to the crack opening.

point a to b the average crack opening associated with point C decreases linearly towards zero.

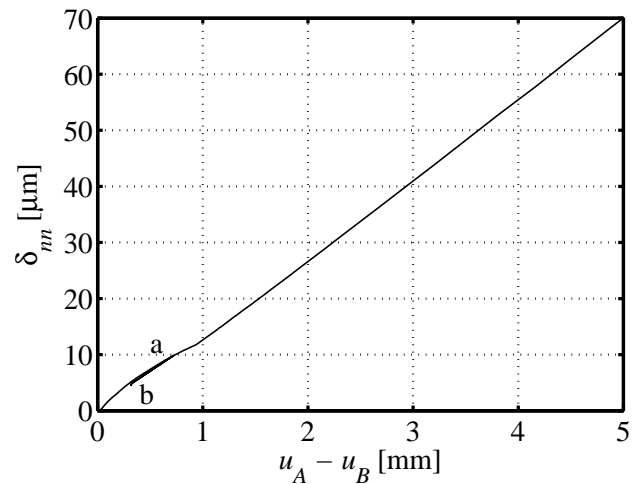


Figure 10: Average crack opening at point C vs. deflection.

The average crack spacing at point C is plotted as a function of the relative deflection in fig. 11. After the first crack is initiated the average crack spacing is 10 mm. The spacing decreases until load point a is reached. During unloading from load point a to b the deflection decreases, but the crack spacing remains constant. After reloading to load point b the crack spacing decreases until a spacing of 2 mm is reached after which the spacing remains constant.

#### 4 CONCLUSIONS

In the present paper a plasticity-based damage mechanics model for Engineered Cementitious Composites (ECC) has been introduced. The present model differs from existing models by combining a matrix and a fiber model in order to describe the behavior of the ECC material. Apart from information about the stress and deformation state the model provides information about crack orientation, opening and spacing. The information provided by the model makes it possible to assess the state of an ECC structure in the serviceability state and to determine the serviceability state limit.

A demonstration of the model has been performed

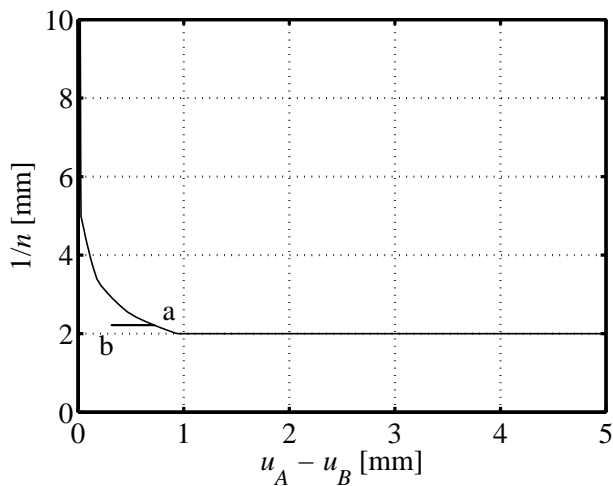


Figure 11: Average crack spacing at point C vs. deflection.

by simulating the behavior of a FPB beam made of ECC. The results obtained from the simulation agreed very well with the experimental results. In addition to global stresses and deformations information about crack traction, opening and spacing was obtained. Even though the example was simple it demonstrated very well the capability of the model.

The cracks in the FPB beam mainly opens in mode I. A test of the mixed mode capability of the model is planned, where results from simulations will be compared with experimental data.

#### References

- Carol, I., P. Prat, and C. López (1997). Normal/shear cracking model: Application to discrete crack analysis. *Journal of Engineering Mechanics* 123(8), 765–773.
- Dick-Nielsen, L., H. Stang, and P. Poulsen (2005). Micro-mechanical analysis of fiber reinforced cementitious composites using cohesive crack modeling. *Knud Hojgaard Conference on Advanced Cement-Based Materials*.
- Dick-Nielsen, L., H. Stang, and P. Poulsen (2006a). Condition for strain-hardening in ECC uniaxial test specimen. *EFC 16. Alexandroupolis, Grækenland 3-7 juli, 2006.*
- Dick-Nielsen, L., H. Stang, and P. Poulsen (2006b). Simulation of strain-hardening in ecc uniaxial test specimen by use of a damage mechanics formulation. *EURO-C 2006 Computational Modelling of Concrete Structures*.
- Han, T., P. H. Feenstra, and S. L. Billington (2003). Simulation of highly ductile fiber-reinforced cement-based composite components under cyclic loading. *ACI Structural Journal* 100(6), 749–757.

- Jirasek, M. (2004). *Modeling of localized Inelastic Deformation*.
- Kabele, P. (2002). Equivalent continuum model of multiple cracking. *Engineering Mechanics (Association for Engineering Mechanics, Czech Republic)* 9 (1/2), 75–90.
- Kesner, K. E. and S. L. Billington (1998). Investigation of ductile cement based composites for seismic strengthening and retrofit. *Concrete Research and Technology*, 19–33.
- Li, V. and C. Leung (1992). Steady state and multiple cracking of short random fiber composites. *ASCE J. Eng. Mech.* 118, 2246–2264.
- Stang, H., J. Olesen, P. Poulsen, and L. Dick-Nielsen (2006). On the application of cohesive crack modeling in cementitious materials. *EURO-C 2006 Computational Modelling of Concrete Structures*.
- Østergaard, L. (2003). Early-age fracture mechanics and cracking of concrete. *Ph.d.-thesis - Technical University of Denmark*.
- Østergaard, L., R. Walter, and J. Olesen (2005). Method for determination of tensile properties for ECC II: Inverse analysis and experimental results. *International Workshop on High Performance Fiber Reinforced Cementitious Composites in Structural Applications*.
- Walter, R., J. Olesen, H. Stang, and T. Vejrums (2006). Analysis of steel bridge deck stiffened with cement-based overlay. *submitted to: ASCE - Journal of Bridge Engineering*.
- Wang, S. and V. Li (2004). Tailoring of pre-existing flaws in ECC matrix for saturated strain hardening. *Ia-FraMCoS*.